Robot Action Planning in the Presence of Careless Humans

Mehdi Hosseinzadeh[®], Senior Member, IEEE, Bruno Sinopoli[®], Fellow, IEEE, and Aaron F. Bobick, Fellow, IEEE

Abstract—This article introduces the notion of carelessness level into robot action planners such that the safety and efficiency are optimized. The core idea is to make the robot's plan less sensitive to the behavior of careless humans who may inattentively violate safety constraints and degrade efficiency. More precisely, our planner reduces the opportunities given to the careless humans to put themselves in danger and hamper the efficiency of the robot's plan. The effectiveness of the proposed planner is demonstrated through simulation studies on a packaging line and on a collaborative assembly line. Results show that the proposed scheme can improve efficiency and safety in both examples.

Index Terms—Action planning, carelessness, human predictive model, human-robot collaboration, receding horizon control.

I. INTRODUCTION

ACKGROUND: Robots are being widely used in a large variety of applications, as a substitute for humans or as an assistant in performing various repetitive, tedious and/or potentially hazardous tasks [1]. While the degree of automation has risen significantly in several industries, a large number of applications require humans to share the workspace with robots [2]. Thus, a safe and efficient human-robot collaboration is a key issue that needs to be addressed [3].

Current methods employed to address safety in shared environments can be classified into two groups: 1) precollision methods, aiming at preventing collisions by either using signals/indicators to alert humans of a potential hazard [4], [5] or by modifying the robot's actions so as to prevent a collision [6], [7], [8], [9] and 2) post-collision methods, aiming at deploying a set of sensors to detect collisions [10], [11], [12], [13], and employ a reaction strategy to minimize harm [14], [15].

Manuscript received 3 December 2023; revised 29 March 2024; accepted 20 May 2024. Date of publication 7 June 2024; date of current version 20 August 2024. This work was supported by the National Science Foundation under Award ECCS-2020289. The work of Mehdi Hosseinzadeh was supported by the WSU Voiland College of Engineering and Architecture. This article was recommended by Associate Editor Z. Liu. (Corresponding author: Mehdi Hosseinzadeh.)

Mehdi Hosseinzadeh is with the School of Mechanical and Materials Engineering, Washington State University, Pullman, WA 99164 USA (e-mail: mehdi.hosseinzadeh@wsu.edu).

Bruno Sinopoli and Aaron F. Bobick are with the Department of Electrical and Systems Engineering and the Department of Computer Science and Engineering, Washington University, St. Louis, MO 63130 USA (e-mail: bsinopoli@wustl.edu; afb@wustl.edu).

This article has supplementary material provided by the authors and color versions of one or more figures available at https://doi.org/10.1109/TSMC.2024.3404346.

Digital Object Identifier 10.1109/TSMC.2024.3404346

In general, pre- and post-collision methods are predominantly reactive. The use of proactive robot action planning methods can improve both safety and efficiency of the collaborative interaction, by first anticipating human actions (see e.g., [16], [17], [18], [19], [20], [21]), and then by scheduling robot's actions accordingly (see e.g., [22], [23], [24], [25], [26], [27]).

Limitations of Prior Work: A large portion of existing action planning schemes are founded on the presumption that the humans are attentive; that is they pay attention to safety rules. However, this presumption is not realistic. Indeed, human error is becoming the prevalent source of accidents in environments shared by humans and robots [28], [29], [30]. Psychological studies have shown that repetitive and tedious works can cause humans to lose attention [31], [32], [33], [34]. Directed attention fatigue [35], [36] and physical fatigue [37], [38] are additional issues that can lead to human errors. Finally, long term exposure to visual/auditory indicators can make them less effective in attracting humans' attentions [39].

Despite the proven negative impact of such loss of attention on both efficiency and safety of robot-human collaboration, carelessness of humans does not play a major role in existing robot action planning schemes. This article attempts to bridge this gap by introducing human carelessness in robot action planning with goal of developing safer and more efficient plans. As far as we know, this is the first attempt to formalize and use such concept to improve robot action planning.

Contribution: Two key contributions of this article are: 1) introduction of a quantifiable notion of carelessness level and 2) development of a learning-based state-of-the-art robot action planning scheme to improve safety and efficiency of robot-human collaboration by leveraging the aforementioned notion. In this article, carelessness is identified with overlooking safety alarms. Accordingly, the carelessness level is a quantity that reflects the likelihood of overlooking a safety alarm; the higher the carelessness level is, the higher is the likelihood that the human will overlook safety alarms.

The main features of the proposed scheme are: 1) it is general and can be applied to any human–robot collaboration satisfying the posed setting; 2) it is modular, meaning that any other objective function or belief update rule can be incorporated into the scheme without changing its structure; 3) carelessness level is automatically and continuously updated by the robot as a result of the observed human's actions, and therefore takes into account possible time-varying effects such as fatigue; and 4) planning policies take safety into

2168-2216 © 2024 IEEE. Personal use is permitted, but republication/redistribution requires IEEE permission. See https://www.ieee.org/publications/rights/index.html for more information.

account, thus avoiding the design of often complex, rarely comprehensive, rule-based, ad-hoc safety rules.

Notation: We denote the set of real numbers by \mathbb{R} , the set of positive real numbers by $\mathbb{R}_{>0}$, and the set of nonnegative real numbers by $\mathbb{R}_{\geq 0}$. Similarly, we denote the set of integer numbers, the set of positive integer numbers, and the set of non-negative integer numbers by \mathbb{Z} , $\mathbb{Z}_{>0}$, and $\mathbb{Z}_{\geq 0}$, respectively. We use $\mathbb{R}_{[a,b]}$ to denote real numbers in interval [a,b]. Given x as a discrete random variable, E[x] represents its expectation; also, we use P(x) to denote the probability density function of x. We use $\mathcal{N}_{[a,b]}(x;\mu,\sigma)$ to indicate that the discrete random variable x conditional on $a \leq x \leq b$ has a truncated normal distribution with mean μ and variance σ . For a given set X, we use |X| to denote its cardinality. For a given set $X = \{(x_1,x_2)|x_1 \in X_1 \text{ and } x_2 \in X_2\}$, $\operatorname{Proj}_{x_1}X = \{x_1 \in X_1 | \exists x_2 \in X_2 \text{ such that } (x_1,x_2) \in X\}$.

II. RELATED WORK

Predictive Human Model: In recent years, there have been several studies on predicting humans' actions/states in the context of human-robot interaction. In some work (e.g., [40]), it is assumed that the robot has complete knowledge about the environment. However, this assumption may not be reasonable in real-world scenarios due to uncertainties in human's behavior. As a result, many researchers have focused on developing a method to enable robots to use the history of humans' actions to predict their future actions and states. In [16], propagation networks have been utilized to detect partially ordered sequential actions of the humans. Albanese et al. [17] introduced the concept of constrained probabilistic Petri nets and showed how this concept can be used to predict humans' actions. In [18], Gaussian mixture distribution techniques have been used to model humans' actions and predict their timing. Markov models have been used in a variety of studies [19], [20], [41] to predict the timing of humans' actions. In [42], an interaction primitive framework for predicting humans' the most likely future movements is developed. The anticipatory temporal conditional random fields have been used in [43] to predict humans' future actions. A Bayesian framework is provided in [44] and [45] to reason about humans' rationality and predict humans' actions. Hawkins and Tsiotras [46] assumed that humans are rational and build a predictive model to anticipate the timing of their actions. In [47] and [48], Bayesian methods are proposed to estimate human motion intention. A two-layer Fuzzy model has been introduced in [49] to understand human's emotional intention. An empirical stochastic transition matrix and a dynamic angle difference exponential have been proposed in [50] to introduce a method for dynamically predicting the human's intention in human-robot environments. In [51], [52], [53], [54], [55], and [56], online Bayesian method has been exploited to infer human's latent states, and hence to generate a predictive model. A convolutional neural network has been proposed in [57] to predict human motion is disassembly tasks. Hwang et al. [58] proposed a dynamic neural network model based on predictive coding to predict human's actions in human-robot interaction. Some *ad hoc* methods (e.g., [21]) have also been proposed.

Robot Action Planning: Once a predictive human model is developed, the robot can use this model to generate a safe and efficient plan. Several robot action planning schemes have been proposed in the literature. Wilcox et al. [59] introduced the adaptive preferences algorithm that computes a flexible optimal policy for robot scheduling and control in assembly manufacturing. In [22], a method has been proposed to optimize the task assignment such that the cycle time is shortened, and consequently the productivity is increased. Probabilistic wait-sensitive task planning have been proposed in [23] and [24] to optimize the robot tasks with respect to the posterior human action distributions, such that the human's total wait time is reduced. Tanaka et al. [25] and Kanazawa et al. [26] proposed a motion planning scheme based on human's trajectory prediction to improve efficiency. In [60], a gradient-based iterative path learning method was proposed to, first, learn the human's motion, and then provide a safe path for the robot. Genetic algorithms have also been utilized in some robot action planners, e.g., [27]. To improve the safety and efficiency of collaborative work, Lyu and Cheah [61] introduced the notion of interactive weight to specify the robot's interaction behaviors based on the human's movements. The notion of the virtual plane is used in [62] for path planning and navigation in dynamic environments. Aoude et al. [63] have developed a path planning framework to safely navigate robots, while avoiding dynamic obstacles with uncertain motion patterns. To make robots assist humans to achieve task-specific objectives, Ranatunga et al. [64] proposed an adaptive scheme that deals with different human dynamics/behaviors. Jiang et al. [65] considered walking-assistant robots and proposes a scheme to enable the robots to adapt to user's motion intent. A contextaware robot action planning has been introduced in [66], where the planning is based on descriptive scenarios describing the expected behavior of agents. Human multirobot interaction has been considered in [67], where a scheme is proposed to plan/modify the robots' actions so to keep the safety above a given threshold. Huo et al. [68] considered wearable robots and proposes an intention-driven method to enable the robot to match the human's action.

III. PROBLEM FORMULATION

In this article, analyses are restricted to the case of one robot interacting with N humans who are not interacting among themselves, as the goal of this article is to introduce the notion of carelessness level. We believe the framework can be generalized to more complex interactions involving several robots and humans interacting and communicating in complex manners, and we plan to tackle this challenge in future work.

Remark 1: When one robot is collaborating with only one human, to improve safety and efficiency, the robot only needs to predict the time instant when the human's state is expected to begin, and to perform the necessary prerequisite action prior to that time instant. This can be done irrespective of the

carelessness level of the human, and is the subject of a large literature, e.g., [23].

A. Collaboration Setting

Consider a collaboration between one robot and N humans (denoted by h_i , $i \in \{1, ..., N\}$), where human h_i repeatedly performs a single task. In this article, time will be discrete and we will use k to denote time instants, where [k, k+1) is equal to $\Delta T \in \mathbb{R}_{>0}$ s. We use the following semantics and notations to describe the setting.

Discrete States: The task of human h_i can be described by Σ_i discrete states, each one describing a particular situation of human h_i . The human h_i should execute a discrete transition (will be discussed later) if a necessary prerequisite action is performed by the robot, and should wait otherwise. Thus, we define additional Σ_i states to describe the gap (i.e., to model waiting periods) between humans' states.

Therefore, the set of all discrete states defined for human h_i is $S_i := \{s_i^1, s_i^{1'}, \dots, s_i^{\Sigma_i}, s_i^{\Sigma_i'}\}$, where $|S_i| = 2\Sigma_i$, s_i^j , $j \in \{1, \dots, \Sigma_i\}$ represent *acting* states, and $s_i^{j'}$, $j \in \{1, \dots, \Sigma_i\}$ represent *waiting* states. For instance, $s_i^{1'}$ means that human h_i has completed s_i^1 and is waiting to begin s_i^2 .

At each time instant, it is assumed that human h_i can be in only one of the discrete states belonging to S_i . Also, we assume that the robot can accurately detect humans' states at all time instants.

Remark 2: Noisy and miscalibrated sensors, occluded vision, and tracking failures can render human's state detection uncertain. By utilizing the methods presented in [23] and [24], it is possible to improve human's state detection results in the presence of noisy and unreliable sensors. We leave the investigation of the behavior of our proposed action planning scheme in the face of human's state detection ambiguity and improving its robustness to future work.

Let ${}^b\tau_i^j$ and ${}^e\tau_i^j$ be two discrete random variables representing the beginning time and ending time of the acting state s_i^j , $j \in \{1, \ldots, \Sigma_i\}$, and ${}^b\tau_i^{j'}$ and ${}^e\tau_i^{j'}$ be two discrete random variables representing the beginning time and ending time of the waiting state $s_i^{j'}$, $j \in \{1, \ldots, \Sigma_i\}$.

the waiting state s_i^j , $j \in \{1, \ldots, \Sigma_i\}$. Discrete Transitions: $\{1, \ldots, \Sigma_i\}$. Discrete transitions for human h_i are $Q_i = \{(s_i^1, s_i^{1'}), (s_i^{1'}, s_i^2), \ldots, (s_i^{\Sigma_i'}, s_i^1)\}$. Discrete transitions are assumed to be instantaneous. Also, similar to [23], we make a Markovian assumption that the beginning of each state is dependent only upon the end of the preceding state; this assumption is reasonable according to the set of discrete transitions Q_i and the fact that human h_i can be in only one of the discrete states at each time instant. Thus, each state begins immediately after the preceding one ends $\{1, \ldots, \infty\}$

$$P\left({}^{b}\tau_{i}^{j+1}|{}^{e}\tau_{i}^{j'}\right) = \begin{cases} 1, & \text{if } {}^{b}\tau_{i}^{j+1} = {}^{e}\tau_{i}^{j'} \\ 0, & \text{otherwise} \end{cases}$$
 (1)

 1 By s_{i}^{j-1} and s_{i}^{j+1} we mean the states before and after s_{i}^{j} . For j=1 we have $s_{i}^{j-1}=s_{i}^{\Sigma_{i}}$, and for $j=\Sigma_{i}$ we have $s_{i}^{j+1}=s_{i}^{1}$. We use the same structure for waiting state $s_{i}^{j'}$, and the beginning and end times of states.

and

$$P\begin{pmatrix} {}^b\tau_i^{j'}|{}^e\tau_i^j \end{pmatrix} = \begin{cases} 1, & \text{if } {}^b\tau_i^{j'} = {}^e\tau_i^j \\ 0, & \text{otherwise.} \end{cases}$$
 (2)

Robot Actions: Let ρ_i^j be a descriptive variable that describes the necessary prerequisite action² for discrete transition $(s_i^{(j-1)'}, s_i^j) \in Q_i, j \in \{1, \dots, \Sigma_i\}$. Thus, we can define the set of robot's actions as $\mathcal{R} = \{\rho_1^1, \dots, \rho_1^{\Sigma_1}, \dots, \rho_N^{I}, \dots, \rho_N^{\Sigma_N}\}$. For safety issues, the robot can perform action ρ_i^j only when human h_i is in a specific subset of the discrete states, which is denoted by T_i^j . This set is a subset of S_i (i.e., $T_i^j \subset S_i$) and contains $2\delta_i^j$ preceding states, i.e., $T_i^j = \{s_i^{j-\delta_i^j}, s_i^{(j-\delta_i^j)'}, \dots, s_i^{j-1}, s_i^{(j-1)'}\}$. When there is no necessary prerequisite action for transition $(s_i^{(j-1)'}, s_i^j) \in Q_i, \rho_i^j$ is null and $T_i^j = S_i - \{s_i^j, s_i^{j'}\}$. See Section III-B for illustrative examples. Plan: A plan is comprised of a sequence of ordered actions to be performed by the robot.

Duration of Discrete States: Regarding the acting state $s_i^j \in S_i$, we specify the conditional dependency via the truncated discrete normal distribution (see [69] for characteristics of a discrete normal distribution). As shown in [23] and [24], truncated discrete normal distributions are proper and effective in modeling human-state timing.

The duration of the acting state s_i^j , $j \in \{1, ..., \Sigma_i\}$ is

$$\mathbf{P}\!\left({}^{e}\boldsymbol{\tau}_{i}^{j}|\,{}^{b}\boldsymbol{\tau}_{i}^{j}\right) \sim \mathcal{N}_{\left[\underline{\lambda}_{i}^{j},\overline{\lambda}_{i}^{j}\right]}\!\left({}^{e}\boldsymbol{\tau}_{i}^{j}-\,{}^{b}\boldsymbol{\tau}_{i}^{j};\,\boldsymbol{\mu}_{i}^{j},\,\boldsymbol{\sigma}_{i}^{j}\right) \tag{3}$$

where μ_i^j and σ_i^j are, respectively, mean and variance, and $\underline{\lambda}_i^j$ and $\overline{\lambda}_i^j$ are truncation limits. We assume that the parameters of (3) are either learned offline or explicitly provided for all i and j. This assumption is plausible, as the parameters can be computed by measuring the duration of humans' states and using distribution fitting techniques.

Remark 3: Using a truncated discrete normal distribution to specify the duration of discrete states is done carefully: 1) it reasonably limits the duration from bottom and above, as tasks have a minimum needed time to complete and cannot last for good and 2) its parameters can be chosen such that it captures possible asymmetric uncertainties, as the uncertainty might be larger in one direction (the state takes longer) than in the other direction (the state takes less). Note that as presented in Section VI, the developed planner uses distribution (3) only to compute the time instants that a state is expected to begin and/or end. Thus, the developed planner can be used in cases where the duration of acting state s_i^j is specified via a different distribution (e.g., uniform and log-normal distributions).

For what concerns the duration of waiting state $s_i^j \in S_i$, $j \in \{1, \ldots, \Sigma_i\}$, let $c_i^{j \to j+1}$ be a binary variable (i.e., $c_i^{j \to j+1} \in \{0, 1\}$), which is one when the prerequisite action ρ_i^{j+1} is performed by the robot and zero otherwise. It is obvious that $c_i^{j \to j+1}$ is always one if ρ_i^{j+1} is null.

 2 It is evident that there is no prerequisite action for discrete transition $(s_i^j, s_i^{j'}) \in Q_i, j \in \{1, \dots, \Sigma_i\}$. Indeed, the waiting state $s_i^{j'}$ begins immediately after the acting state s_i^{j} ends.

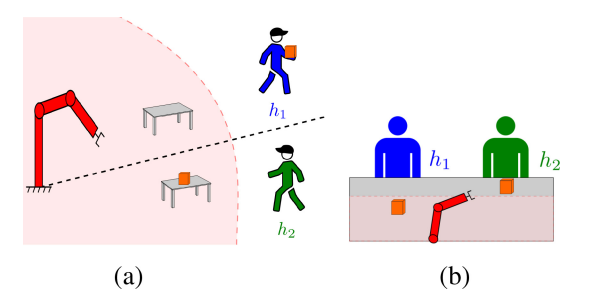


Fig. 1. Two applications satisfying the described setting. (a) Packaging line, where a robot provides boxes for humans. (b) Collaborative assembly, where a robot provides assembly pieces for humans.

When $c_i^{j \to j+1} = 1$, human h_i proceeds³ by ending the waiting state $s_i^{j'}$. When $c_i^{j \to j+1} = 0$, an alarm/signal must be triggered to alert human h_i to the danger. In this case, human h_i should not proceed until the time that the robot performs the required action and the alarm goes off. However, human h_i may inattentively violate the safety constraints by overlooking the safety alarms. We use $\alpha_i \in \mathbb{R}_{[0,1]}$ to specify the likelihood that human h_i overlooks the safety alarms. If $\alpha_i = 1$, human h_i violates the safety constraints almost surely. If $\alpha_i = 0$, human h_i is attentive and does not violate the safety constraints. Thus, the overall distribution for the duration of the waiting state $s_i^{j'} \in S_i$, $j \in \{1, \ldots, \Sigma_i\}$ should incorporate the information about $c_i^{j \to j+1}$ and α_i (in Section VI, the developed planner incorporates this information only with respect to the current time).

B. Illustrative Examples

Many real-world human–robot collaborations meet the setting presented in Section III-A. Here, we use two examples to illustrate the setting: 1) packaging line [Fig. 1(a)] and 2) collaborative assembly [Fig. 1(b)].

1) Packaging Line: Each human picks up a box from a pick-up table and puts it on a delivery table. For human h_i , we define the following discrete states: s_i^1 : "being inside the red region, including walking toward the pick-up table, picking up the box, and walking away from the pick-up table;" $s_i^{1'}$: "waiting inside the red region before exiting;" s_i^2 : "being outside the red region, including walking toward the delivery table, putting the box on the delivery table, and walking away from the delivery table;" and $s_i^{2'}$: "being outside the red region and waiting for the robot to put a box on the pick-up table." Regarding the robot actions, ρ_i^1 is "putting a box on the pick-up table associated with human h_i ," and $\rho_i^2 \ \forall i$ is null. To ensure safety, the robot should not perform action ρ_i^1 when human h_i is inside the red region, meaning that $T_i^1 = \{s_i^2, s_i^2'\}$.

2) Collaborative Assembly: A robot provides η assembly pieces for each human. For human h_i , we define the following discrete states: s_i^1 : "hands (one or both) inside the red region to pick up the first piece;" $s_i^{1'}$: "waiting inside the red region after picking up the first piece;" s_i^2 : "hands outside the red region to fit the first piece;" s_i^2 : "waiting for the second piece to be

³Note that once human h_i executes transition $(s_i^{j'}, s_i^{j+1}) \in Q_i$, the binary variable $c_i^{j \to j+1}$ becomes zero again for future events.

delivered ...; " $s_i^{2\eta-1}$: "hands inside the red region to pick up the η th piece;" $s_i^{(2\eta-1)'}$: "waiting inside the red region after picking up the η th piece;" $s_i^{2\eta}$: "hands outside the red region to fit the η th piece;" and $s_i^{(2\eta)'}$: "waiting for the first piece to be delivered." The necessary condition for discrete transitions $(s_i^{(2\eta)'}, s_i^1) \in Q_i$, ..., $(s_i^{(2\eta-2)'}, s_i^{2\eta-1}) \in Q_i$ is, respectively, providing the first, ..., and η th pieces. Thus, $\rho_i^2, \ldots, \rho_i^{2\eta} \forall i$ are null, and $\rho_i^1, \ldots, \rho_i^{2\eta-1}$ are the action of providing the appropriate assembly pieces for human h_i . To ensure safety, the robot should not perform any action if the hands of human h_i are inside the red region. Thus, $T_i^1 = \{s_i^{2\eta}, s_i^{(2\eta)'}\}, \ldots$, and $T_i^{2\eta-1} = \{s_i^{2\eta-2}, s_i^{(2\eta-2)'}\}$.

C. Goal of This Article

As mentioned in Section III-A, to ensure safety of the robot and humans, the robot can perform action ρ_i^j only when human h_i is in T_i^j (more precisely, when human h_i is in one of the states belonging to T_i^j), which does not include the acting state s_i^j (since ρ_i^j is a prerequisite action for state s_i^j). Thus, when the robot has not performed the necessary action ρ_i^j , inattentively overlooking the safety alarms and executing the discrete transition $(s_i^{(j-1)'}, s_i^j) \in Q_i$ (i.e., disregarding the waiting state $s_i^{(j-1)'}$ and immediately beginning the acting state s_i^j) is a hazard to human h_i and the robot. Moreover, such a careless behavior disturbs the robot's plan, and consequently degrades the efficiency.

The goal of this article is to develop a robot action planning scheme that is less sensitive to the behavior of careless humans. More precisely, the developed planner reduces the opportunities given to the careless humans to put themselves in danger and hamper the efficiency of the robot's plan. The proposed scheme has three components: 1) a predictive human model to anticipate the timing of humans' states; 2) a belief update unit to update the robot's belief about the carelessness of each human; and 3) a planning unit to determine the next action of the robot. These components will be discussed separately in the following sections.

IV. HUMAN PREDICTIVE MODEL

Taking the inspiration from [23] and [24], this section develops a predictive model for human h_i . Given the time instant k, consider the prediction horizon [k, k + K], where $K \in \mathbb{Z}_{>0}$ is the prediction length. Assuming that human h_i is in state s_i^j at time instant k, Fig. 2 shows a schematic Bayes network of states of human h_i within the prediction horizon, where $G \in \mathbb{Z}_{>0}$ is the number of future acting states within the prediction horizon

To build a predictive model to predict the behavior of human h_i within the prediction horizon [k, k+K], analogous to [23] and [24], we *optimistically* assume that within this horizon the robot is able to perform every necessary action with perfect timing; i.e., $c_i^{j \to j+1} = 1 \ \forall i, j$ within the prediction horizon.

Remark 4: Due to human-state timing and robot-action timing, in practice, the robot may not be able to perform necessary

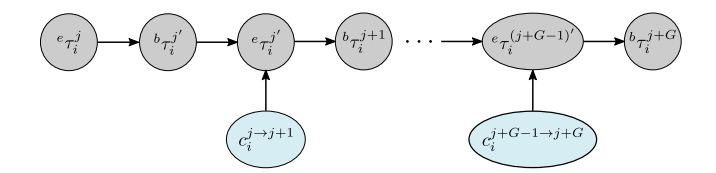


Fig. 2. Bayes network representing the states of human h_i within a prediction horizon, assuming that human h_i is in state s_i^j at time instant k.

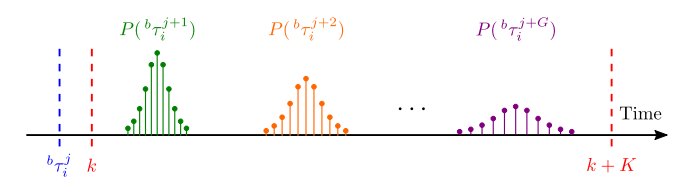


Fig. 3. Action times of human h_i within a prediction horizon.

prerequisite actions with perfect timing. For instance, when humans are much faster than the robot, delays in performing the prerequisite actions is inevitable. The developed planner in Section VI uses the receding horizon control strategy [70], which allows the robot to take into account these delays in determining the plan. Thus, the impacts of the abovementioned optimistic assumption will be compensated by the developed planner. Even though this approach is only suboptimal (like any other receding horizon-based scheme with such simplifying assumptions about future [71]), our numerical experiments suggest that it works well. Future research will investigate how to anticipate these delays and include them in robot action planners.

Under the above-mentioned optimistic assumption (i.e., $c_i^{j \to j+1} = 1 \ \forall i, j$ within the prediction horizon [k, k+K]), the probability density function of the beginning time of human h_i 's states can be computed via the following recursion:

$$\begin{split} &P\left({}^{b}\tau_{i}^{j+1}\right) \propto \sum_{e_{\tau_{i}}^{j'}} \sum_{b_{\tau_{i}}^{j'}} \sum_{e_{\tau_{i}}^{j}} \sum_{b_{\tau_{i}}^{j}} P\left({}^{b}\tau_{i}^{j+1} | {}^{e}\tau_{i}^{j'}\right) \cdot \\ &P\left({}^{e}\tau_{i}^{j'} | {}^{b}\tau_{i}^{j'}\right) \cdot P\left({}^{b}\tau_{i}^{j'} | {}^{e}\tau_{i}^{j}\right) \cdot P\left({}^{e}\tau_{i}^{j} | {}^{b}\tau_{i}^{j}\right) \cdot P\left({}^{b}\tau_{i}^{j}\right) \end{aligned} \tag{4}$$

where the sum is over all possible values of ${}^b\tau_i^j, \; {}^e\tau_i^j, \; {}^b\tau_i^{j'}, \;$ and ${}^e\tau_i^{j'}$. In (4), $P({}^b\tau_i^{j+1}|{}^e\tau_i^{j'})$ is as in (1), $P({}^b\tau_i^{j'}|{}^e\tau_i^{j})$ is as in (2), $P({}^e\tau_i^{j}|{}^b\tau_i^{j})$ is as in (3), and ${}^b\tau_i^{j}$ is known for the current state of human h_i . Also, under the above-mentioned optimistic assumption, the distribution for the duration of waiting state $s_i^{j'} \in S_i$ within the prediction horizon is 4

$$P\left({}^{e}\tau_{i}^{j'} \mid {}^{b}\tau_{i}^{j'}\right) = \begin{cases} 1, & {}^{e}\tau_{i}^{j'} = {}^{b}\tau_{i}^{j'} \\ 0, & \text{otherwise.} \end{cases}$$
 (5)

Note that the recursion given in (4) should be computed for every ${}^b\tau_i^{j+1} \in [k,k+K]$. Thus, the computational complexity of (4) is $O(G \cdot (K+1)^2)$. Fig. 3 demonstrates the probability density functions computed via (4). From this figure, as we look further in the future, the distributions become wider so that it has less precision but higher recall.

V. HUMANS' CARELESSNESS LEVEL

Assuming that all humans always pay attention to safety alarms, one can use existing planners (e.g., [23], [26]) to

⁴Since $c_i^{j\to j+1}$ is assumed to be one within the prediction horizon, the predictive model (4) does not incorporate the information about α_i , as $c_i^{j\to j+1}=1$ means that human h_i is not given the opportunity to overlook the safety alarms. In Section VI, our planner considers the carelessness of humans in determining the robot's actions. Future research will investigate how to effectively incorporate the information about α_i in the model (4).

determine a plan for the robot based on the human predictive model given in (4). However, the efficiency of such plans can be largely degraded if one (or more) human overlooks the safety alarms inattentively. Note that such a careless behavior is a hazard to the robot and human as well. To address this issue, we introduce the notion of carelessness level of humans. We will see in Section VI how to incorporate carelessness of humans into robot planners to provide safe and efficient plans.

Intuitively, the carelessness level of human h_i is the robot's belief about the likelihood that human h_i overlooks the safety alarms. Indeed, the carelessness level of human h_i should estimate α_i described in Section III. However, it is unsurprisingly difficult to learn the value of α_i just by observing the behavior of human h_i , as the humans' behavior may not encode sufficient information about their carelessness level; indeed, human h_i may never face a safety alarm.

In Section VI, our planner reduces the duration of wait states for all humans, while prioritizing careless over attentive humans. Such prioritization reduces the opportunities given to careless humans to make the robot deviate from its plan. Thus, our planner requires only *relative* carelessness levels to determine a prioritization order. More specifically, the robot only needs to arrange the humans in order of how much careless they were about safety alarms in the past. Though we do not claim to be optimal, our numerical experiments suggest that generating a prioritization order based on humans' behavior in the past can improve safety and efficiency metrics.

Let $\beta_i(k) \in \mathbb{R}_{[0,1]}$ be the relative carelessness level of human h_i at time instant k. The relative carelessness level $\beta_i(k)$ can be computed as follows:

$$\beta_i(k) = \begin{cases} \frac{V_i(k-1)}{\sum_{j=1}^N V_j(k-1)}, & \text{if } \sum_{j=1}^N V_j(k-1) > 0\\ \frac{1}{N}, & \text{if } \sum_{j=1}^N V_j(k-1) = 0 \end{cases}$$
(6)

where $V_i(k-1) \in \mathbb{Z}_{\geq 0}$ is the number of safety violations by human h_i until the time instant k-1.

Remark 5: In this article, we assume that the carelessness level α_i for human h_i is constant, and consequently the number of careless humans remain unchanged during the collaboration. This assumption might not be realistic in real-world scenarios, as carelessness level (which reflects the likelihood of overlooking a safety alarm) involves many psychological and behavioral aspects that can change during the collaboration. We leave studying such cases to future research; future work will consider how to obtain or identify the carelessness level of humans.

VI. ROBOT ACTION PLANNING SCHEME

In this section, we develop an optimal robot action planning scheme which takes into account humans' carelessness. The developed scheme should be run only at planning instants in which the robot is ready to begin performing a new action. We use k_p to denote the planning instants. Thus, at any planning instant k_p , the robot determines a sequence of ordered actions. The robots uses the receding horizon control strategy [70] for this purpose; that is, the robot optimizes the future actions using the predictions in the horizon, but only decides the next action and then optimizes again, repeatedly.

A. Duration of the Robot's Actions

Let $\ell_i^J \in \mathbb{Z}_{\geq 0}$ be the required time for the robot to complete performing action ρ_i^J . Note that $\ell_i^J = 0$ if ρ_i^J is null, and $\ell_i^J \in \mathbb{Z}_{>0}$ otherwise.

B. Set of Admissible Robot Actions

Let $\mathcal{M}(k_p) \subset \mathcal{R}$ be the set of all non-null actions that should be considered by the planner at the planning instant k_p . This set will be referred as the set of admissible robot actions at planning instant k_p . To determine the set $\mathcal{M}(k_p) \subset \mathcal{R}$, the robot needs to, first, identify humans whose states at the planning instant k_p are safe,⁵ and then determine the first upcoming transition with non-null prerequisite action for every identified human.

Note that at any planning instant k_p , the number of humans whose states are safe is less or equal to the total number of humans collaborating with the robot. Also, note that $\mathcal{M}(k_p)$ includes only one action associated with each human whose state is safe. Therefore, $|\mathcal{M}(k_p)| \leq N \ \forall k_p$.

The set of pairs of humans and their demanded prerequisite actions is defined as follows:

$$\mathcal{I}(k_p) = \{(i,j) | \rho_i^j \in \mathcal{M}(k_p) \} \tag{7}$$

where $\operatorname{Proj}_i \mathcal{I}(k_p)$ gives the set of humans whose states at planning instant k_p are safe (or the set of humans to be considered at the planning instant k_p). It is evident that $|\operatorname{Proj}_i \mathcal{I}(k_p)| = |\mathcal{M}(k_p)| \leq N \ \forall k_p$.

C. Expected Time Interval to Begin the Admissible Action ρ_i^J

Given $\mathcal{M}(k_p)$ as the set of admissible actions at planning instant k_p , the probabilistic predictive model given in (4) can be utilized to determine an *expected* time interval that the robot should begin performing the admissible non-null action $\rho_i^j \in \mathcal{M}(k_p)$ sometime within that interval to complete performing that action before the time that human h_i is expected to begin the acting state $s_i^j \in S_i$.

Remark 6: Since any theoretical guarantee depends on the model it is based on, safety guarantees will inherit the probabilistic nature of human predictive model described in Section IV. Thus, the planning scheme will need to determine

an action plan which is predicted/expected to be safe. To the best of our knowledge, this is an issue in robot action planning schemes which are developed based upon probabilistic predictive human models; see e.g., [44], [45], [63], [72], [73].

The expected time interval for the admissible non-null action $\rho_i^j \in \mathcal{M}(k_p)$ is represented by $[\underline{x}_i^j, \overline{x}_i^j]$, where \underline{x}_i^j is the time that the robot is allowed to begin performing action ρ_i^j without any safety issues and \overline{x}_i^j is the time that the robot should complete performing ρ_i^j to prevent possible safety issues. Regarding \underline{x}_i^j , according to Section III two cases can happen.

- 1) The Current State of Human h_i Is in T_i^j : In this case, \underline{x}_i^j is the time instant that the state of human h_i has entered the set T_i^j . This time is the beginning time of the acting state $s_i^{j-\delta_i^j}$, which is denoted by ${}^b\tau_i^{j-\delta_i^j}$. Note that in this case, ${}^b\tau_i^{j-\delta_i^j}$ is a known time instant in the past.
- 2) The Current State of Human h_i Is Not in T_i^j : In this case, \underline{x}_i^j is the time instant that the state of human h_i is expected to enter the set T_i^j . In other words, \underline{x}_i^j is equal to the time that human h_i is expected to begin acting state $s_i^{j-\delta_i^j}$.

For what regards \bar{x}_i^j , since ℓ_i^j is the time required for the robot to complete action ρ_i^j , \bar{x}_i^j should be ℓ_i^j time instants before the time that human h_i is expected to exit from the set T_i^j (i.e., the time that human h_i is expected to begin the acting state s_i^j).

Therefore, according to the above-mentioned discussion, \underline{x}_i^j and \overline{x}_i^j can be computed as

$$\underline{x}_{i}^{j} = \begin{cases} b \tau_{i}^{j-\delta_{i}^{j}}, & \text{if human } h_{i} \text{ is in } T_{i}^{j} \\ E b \tau_{i}^{j-\delta_{i}^{j}}, & \text{otherwise} \end{cases}$$
(8)

$$\overline{x}_i^j = E \left[{}^b \tau_i^j \right] - \ell_i^j \tag{9}$$

where ℓ_i^j is as in Section VI-A, T_i^j and δ_i^j are as in robot actions in Section III-A, and $E[{}^b\tau_i^{j-\delta_i^j}]$ and $E[{}^b\tau_i^j]$ can be computed according to the distributions determined in (4). Note that ${}^b\tau_i^{j-\delta_i^j}$ is known if human h_i is in T_i^j . See Fig. 4 for an illustration of the expected time interval $[x_i^j, \bar{x}_i^j]$.

Remark 7: The prediction horizon K should be selected such that it can cover at least G future acting states for all humans, where G should be selected such that the expected time interval to begin the admissible action ρ_i^j can be computed via (8) and (9). Since G depends on application (for instance, G=3 is sufficient for packaging line and collaborative assembly examples presented in Sections VII and VIII), the prediction horizon K will depend on application as well. It should be remarked that using a small K can prevent us from implementing the proposed scheme as it would be impossible to compute the interval (8) and (9), and using a large K can unnecessarily increase the computational complexity as the computational complexity of (5) is $O(G \cdot (K+1)^2)$.

⁵Assuming that the robot can accurately detect the state of humans (see Remark 2), the robot does that by excluding humans whose states are *potentially* unsafe. See "Robot Actions" in Section III-A for more details about safe and potentially unsafe states.

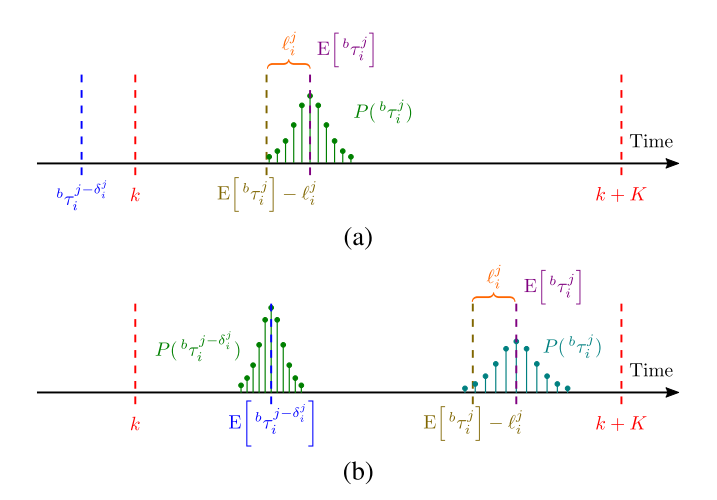


Fig. 4. Illustration of the expected time interval $[\underline{x}_i^j, \overline{x}_i^j]$ in which the robot should begin performing the non-null admissible action $\rho_i^j \in \mathcal{M}(k_p)$. (a) Human h_i is in T_i^j and (b) human h_i is not in T_i^j .

D. Robot Planner

Given $\mathcal{M}(k_p)$ as the set of admissible actions at planning instant k_p , the plan can be represented by means of the beginning time of the admissible actions.

beginning time of the admissible actions. Let $x = [x_i^j] \in \mathbb{Z}_{\geq 0}^{|\mathcal{M}(k_p)|}$, where x_i^j , $(i,j) \in \mathcal{I}(k_p)$ is the time that the robot should begin performing the admissible nonnull action ρ_i^j . Also, let $\underline{x} = [\underline{x}_i^j] \in \mathbb{Z}_{\geq 0}^{|\mathcal{M}(k_p)|}$ and $\overline{x} = [\overline{x}_i^j] \in \mathbb{Z}_{\geq 0}^{|\mathcal{M}(k_p)|}$, where \underline{x}_i^j are as in (8) and (9), respectively. Let $\beta = [\beta_i(k_p)] \in \mathbb{R}_{[0,1]}^{|\mathcal{M}(k_p)|}$, where $\beta_i(k_p)$, $i \in \text{Proj}_i \mathcal{I}(k_p)$ is as in (6).

The beginning time for performing the non-null admissible actions at the planning instant k_p can be computed via the following constrained optimization problem:

$$x^* = \arg \min_{\substack{x \in \mathbb{Z}_{>0}^{|\mathcal{M}(k_p)|}}} f(\beta, x, \underline{x}, \overline{x})$$
 (10)

subject to

$$x_i^j \ge \max\{\underline{x}_i^j, k_p\} \ \forall (i, j) \in \mathcal{I}(k_p)$$
 (11)

and

$$\begin{cases} x_{i_{2}}^{j_{2}} \geq x_{i_{1}}^{j_{1}} + \ell_{i_{1}}^{j_{1}}, & \text{if } x_{i_{2}}^{j_{2}} > x_{i_{1}}^{j_{1}} \\ x_{i_{1}}^{j_{1}} \geq x_{i_{2}}^{j_{2}} + \ell_{i_{2}}^{j_{2}}, & \text{if } x_{i_{2}}^{j_{2}} < x_{i_{1}}^{j_{1}} \end{cases} \forall (i_{1}, j_{1}), (i_{2}, j_{2}) \in \mathcal{I}(k_{p}).$$

$$(12)$$

Remark 8: $|\mathcal{M}(k_p)|$ is not constant during the collaboration, which means that the dimension of the decision variable x is not constant. Note that this does not cause any issue, as the robot performs only the first action of each plan, and solves a new optimization problem in the next planning instant.

The cost function $f(\cdot)$ as in (10) should be defined so as to accomplish the goal of reducing the duration of waiting states for all humans, while prioritizing careless ones. Note that reducing the wait time, which has been widely used in the literature (e.g., [23], [24], [25], [26], [74]), implies that the prerequisite actions are performed in time, which improves safety and efficiency, as it reduces the opportunities given to

the careless humans to put themselves in danger and degrade the efficiency of the robot's plan.

The following cost function is proposed:

$$f(\beta, x, \underline{x}, \overline{x}) = \theta_1 f_1(\beta, x, \underline{x}, \overline{x}) + \theta_2 f_2(\beta, x, \underline{x}, \overline{x})$$
(13)

where $\theta_1, \theta_2 \in \mathbb{R}_{>0}$ are weighting parameters, the objective function $f_1(\beta, x, \underline{x}, \overline{x})$ forces the robot to begin performing the admissible non-null actions as soon as possible, and the objective function $f_2(\beta, x, \underline{x}, \overline{x})$ penalizes completing performing the admissible non-null actions after the time that is expected to be potentially unsafe.

The following objective functions are proposed:

$$f_1(\beta, x, \underline{x}, \overline{x}) = \sum_{(i,j)\in\mathcal{I}(k_p)} \beta_i(k_p) \left(x_i^j - \underline{x}_i^j\right)^2 \tag{14}$$

$$f_2(\beta, x, \underline{x}, \overline{x}) = \sum_{(i,j)\in\mathcal{I}(k_p)} e^{-\beta_i(k_p)\left(\overline{x}_i^j - x_i^j\right)}$$
(15)

which prioritize careless humans, as $\beta_{i_1}(k_p)$, $i_1 \in \{1, ..., N\}$ is greater than $\beta_{i_2}(k_p)$, $i_2 \in \{1, ..., N\}$ if the robot believes that human h_{i_1} is more careless than human h_{i_2} [see (6)].

Remark 9: According to (13), we can interpret θ_i , $i \in \{1, 2\}$ as the weight we attach to the objective function $f_i(\cdot)$. In particular, we can [75] interpret the ratio θ_1/θ_2 as the relative weight or relative importance of the objective function $f_1(\cdot)$ compared to the objective function $f_2(\cdot)$. Based on this insight, the weights θ_1 and θ_2 can be determined by using techniques described in, e.g., [76], [77].

Remark 10: Although we make no claim that minimizing the cost function given in (13) with objective functions given in (14) and (15) is ideal or unique, our numerical experiments suggest that such a cost function with the carelessness level incorporated into yields reasonable results.

Constraint (11) ensures that the robot can begin performing the admissible action ρ_i^j only when it is expected to be safe, which should be after k_p . Constraint (12) ensures that the robot cannot perform two actions simultaneously.

Remark 11: Optimization problem (10)–(12) with cost function $f(\cdot)$ as in (13)–(15) is a nonconvex mixed-integer nonlinear programming problem, as the decision variable x_i^j is integer, objective functions (14) and (15) are nonlinear, and (12) is nonconvex.

After computing $(x_i^J)^* \ \forall (i,j) \in \mathcal{I}(k_p)$ by solving the constrained optimization problem (10)–(12), the robot begins performing the action $\rho^*(k_p)$ which can be determined as follows:

$$\rho^*(k_p) = \left\{ \rho_{i^*}^{j^*} \in \mathcal{M}(k_p) \middle| (i^*, j^*) = \arg \min_{(i,j) \in \mathcal{I}(k_p)} (x_i^j)^* \right\}.$$
(16)

E. Robot Action Planning Algorithm

The robot action planning algorithm is presented in Algorithm 1. The corresponding pseudocode is given in Algorithm 2. This algorithm should be run at every planning instant to schedule the robot's future actions. Note that though Algorithm 1 should be run at every planning instant, the robot should compute $\beta_i \ \forall i$ given in (6) at every time instant.

Algorithm 1 Robot Action Planning Scheme

Input: Humans' states and relative carelessness levels.

Output: The robot's action at k_p (i.e., $\rho^*(k_p)$).

1: Determine the set of admissible actions $\mathcal{M}(k_p)$.

2: Determine the sets $\mathcal{I}(k_p)$ and $\operatorname{Proj}_i \mathcal{I}(k_p)$.

3: Compute the distribution (4) for all $i \in \operatorname{Proj}_i \mathcal{I}(k_p)$.

4: Determine \underline{x}_i^j and \overline{x}_i^j via (8) and (9) for all $\rho_i^j \in \mathcal{M}(k_p)$.

5: Solve optimization problem (10)-(12) and compute x^* .

6: Determine $\rho^*(k_p)$ as in (16).

Algorithm 2 Pseudocode of the Proposed Robot Action Planning Scheme

```
Input: s_i and \beta_i for all i
   1: \mathcal{M} \leftarrow \{\}
  2: \mathcal{I} \leftarrow \{\}
  3: \text{Proj}_{i}\mathcal{I} \leftarrow \{\}
  4: P \leftarrow \{\}
  5: for i \leftarrow 1 to N do
              for j \leftarrow 1 to \sum_i do if s_i = s_i^{(j-1)'} then
  7:
                          \mathcal{M} \leftarrow \rho_i^j\mathcal{I} \leftarrow (i, j)
  8:
   9:
                          \text{Proj}_i \mathcal{I} \leftarrow i
 10:
                     end if
 11:
               end for
12.
 13: end for
 14: for i \in \text{Proj}_i \mathcal{I} do
             for {}^{b}\tau_{i}^{j+1} \leftarrow k \text{ to } k+K \text{ do}
P \leftarrow P({}^{b}\tau_{i}^{j+1})
 15:
 16:
               end for
 17:
 18: end for
19: for \rho_i^j \in \mathcal{M} do
20: \underline{x}_i^j \leftarrow \begin{cases} b \tau_i^{j-\delta_i^j}, & \text{if human } h_i \text{ is in } T_i^j \\ E[b \tau_i^{j-\delta_i^j}], & \text{otherwise} \end{cases}
21: \bar{x}_i^j \leftarrow E[b\tau_i^j] - \ell_i^j
22: end for
23: x^* \leftarrow \arg \min f(\beta, x, x, \overline{x})
24: (i^*, j^*) \leftarrow \arg\min(x_i^j)^*
25: return \rho^*
```

VII. SIMULATION STUDY—PACKAGING LINE

In order to demonstrate the effectiveness of the proposed robot action planning scheme given in Algorithm 1, we simulated a human–robot collaboration on a packaging line with four humans; see Section III-B for details. Note that our focus in this section was on algorithmic and analytical aspects of the proposed robot action planning scheme on a simplistic, but yet realistic, application. We leave the evaluation of the proposed robot action planning scheme with real humans to future work.

System parameters were
$$\mu_1^1 = \mu_4^1 = 4$$
, $\mu_2^1 = \mu_3^1 = 6$, $\mu_1^2 = \mu_2^2 = 8$, $\mu_3^2 = \mu_4^2 = 10$, $\underline{\lambda}_1^1 = \underline{\lambda}_4^1 = 3$, $\overline{\lambda}_1^1 = \overline{\lambda}_4^1 = \underline{\lambda}_2^1 = \underline{\lambda}_3^1 = 5$, $\underline{\lambda}_1^2 = \overline{\lambda}_2^1 = \underline{\lambda}_2^2 = \overline{\lambda}_3^1 = 7$, $\overline{\lambda}_1^2 = \overline{\lambda}_2^2 = \underline{\lambda}_3^2 = \underline{\lambda}_4^2 = 9$,

 $\overline{\lambda}_3^2 = \overline{\lambda}_4^2 = 11$, $\sigma_1^1 = \sigma_1^2 = \sigma_4^1 = \sigma_4^2 = 0.5$, $\sigma_2^1 = \sigma_2^2 = \sigma_3^1 = \sigma_3^2 = 1.5$, K = 30, and $\ell_i^j = 3 \ \forall i,j$. We assumed that objective functions $f_1(\cdot)$ and $f_2(\cdot)$ are equally important; hence, we set $\theta_1 = \theta_2 = 1$. For the considered collaboration, G = 3 is sufficient to compute the expected time intervals as in (8) and (9). We assumed that α for careless humans is 0.5, i.e., the probability that a careless human overlooks safety alarms is 50%; see Section VII-C for a sensitivity analysis of the performance metrics with respect to the value of this parameter.

If the robot's action is interrupted inattentively, the robot goes to the source point (which is assumed to be safe) and determines a new plan. We assumed that the required time for the robot to reach the source point is equal to the time spent on performing the action before interruption. Note that although, in practice, the required time for the robot to reach the source point depends on the robot's dynamics, and can be larger or smaller than the time spent on performing the action before interruption, the above-mentioned assumption has been made only for simulation purposes without violating the realisticity of the problem setting.

The MIDACO⁶ solver [78] was used to solve the constrained optimization problem (10)–(12). The simulations were run on an Intel Core i7-7500U CPU 2.70 GHz with 16.00 GB of RAM. The mean computation time was 0.2437 s, which is largely acceptable for real-time implementation.

For comparison purposes, we simulated two strawman schemes.

- 1) SS#1 [23]: The case where $\beta_1(k) = \beta_2(k) = \beta_3(k) = \beta_4(k) = 0.25 \, \forall k$ (i.e., an optimal planner that does not consider carelessness of humans and treats all humans equally regardless of their carelessness level).
- 2) SS#2 [79]: A periodic schedule where the robot serves human h_1 , then human h_2 , then human h_3 , then human h_4 , and repeats this cycle.

Note that these schemes do not consider carelessness level of humans (to the best of our knowledge, there is no scheme in the literature that considers carelessness aspect of humans), and the presented comparison study aims at showing the impact of incorporating the carelessness aspect of humans in robot action planners.

To have a visual demonstration of the considered human–robot collaboration, a simulator was generated. A video of operation of the generated simulator is available at the following address: https://youtu.be/_MIBWfJVFFc. Also, time profile of $\beta_i(k)$ $\forall i$ for a typical collaboration is shown in Fig. 5.

To provide a quantitative analysis, we considered 2000 experiments, where for each experiment the initial state of human h_i is uniformly selected from the set $\{s_i^1, s_i^{1'}, s_i^2, s_i^{2'}\} \forall i$. Also, for each experiment, the combination of careless humans

⁶Mixed integer distributed ant colony optimization (MIDACO) is a numerical high-performance software for solving nonconvex mixed-integer nonlinear programming problems, which does not require the objective functions and constraints to be given in explicit mathematical form. Note that although MIDACO does not provide a guarantee to reach the global optimal solution, our numerical experiments demonstrated that MIDACO can effectively obtain the global optimal solution for problem (10)–(15).

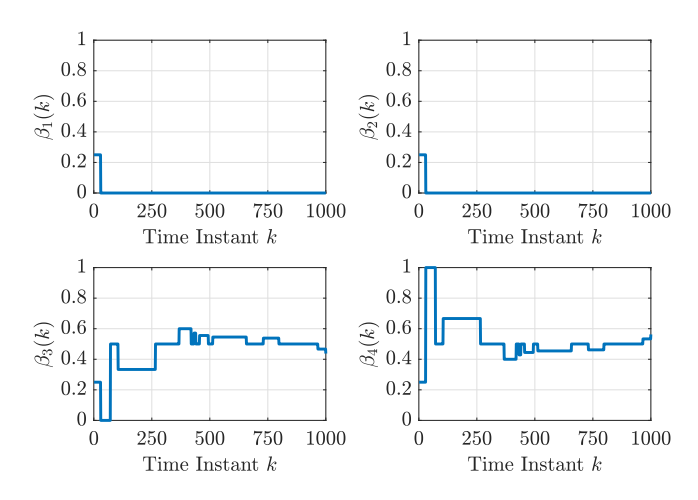


Fig. 5. Packaging line—time profile for $\beta_i(k) \, \forall i$ for a typical collaboration, where humans h_3 and h_4 are careless with the same likelihood of overlooking the safety alarms.

is randomly selected from the set of all possible combinations; for instance, when there are three careless humans, we select the combination of careless humans randomly from the set $\{h_1, h_2, h_3\}, \{h_1, h_2, h_4\}, \{h_1, h_3, h_4\}, \{h_2, h_3, h_4\}\}.$

A. Efficiency Assessment

Let define the efficiency as

Efficiency =
$$\left(1 - \frac{\text{Total Wait Time}}{\text{Collaboration Time}}\right) \times 100$$
 (17)

where "Total Wait Time" is the wait time of all humans. The statistics of the achieved efficiency by the strawman schemes and the proposed robot action planning scheme is compared in Fig. 6. As seen in Fig. 6, across all cases, the proposed robot action planning scheme has 10.25% mean (up to 34.37%) gain over SS#1, and 21.25% mean (up to 36.15%) gain over SS#2 with respect to efficiency.

Fig. 6 reveals that existence of a single careless human can degrade (on mean) the efficiency of strawman schemes SS#1 and SS#2 by 11.71% and 25.03%, respectively. While the degradation for the proposed planner is only 0.86%. This underlines the importance of considering the carelessness of humans in robot action planners, as presuming that humans are attentive and pay attention to safety alarms is not realistic in real-world human–robot collaborations.

B. Safety Assessment

To compare safety performance, we considered the number of safety issues (i.e., the number of safety violations) per 100 time instants (which represents the rate of safety issues). Statistics are provided in Fig. 7. Note that the case where there is no careless human is not shown in Fig. 7, as there will be no safety issue regardless of the employed scheme. As seen in Fig. 7, across all cases, the proposed robot action planning scheme has 72.61% mean (up to 100%) gain over SS#1, and 78.85% mean (up to 100%) gain over SS#2 with respect to safety.

Note that as the number of careless humans increases, the variance of the efficiency (see Fig. 6) and safety (see

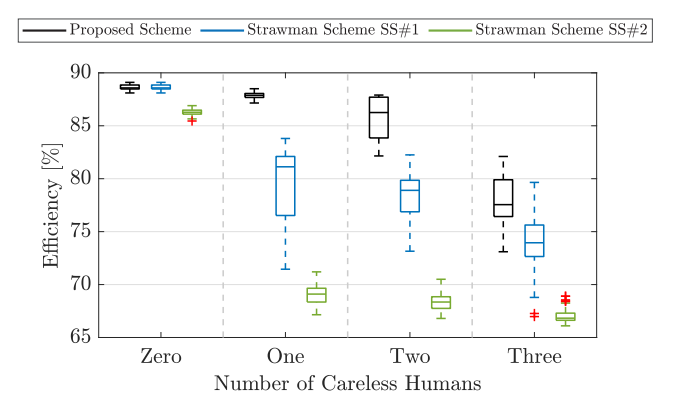


Fig. 6. Packaging line—comparing efficiency for the proposed scheme, the strawman scheme SS#1, and the strawman scheme SS#2.

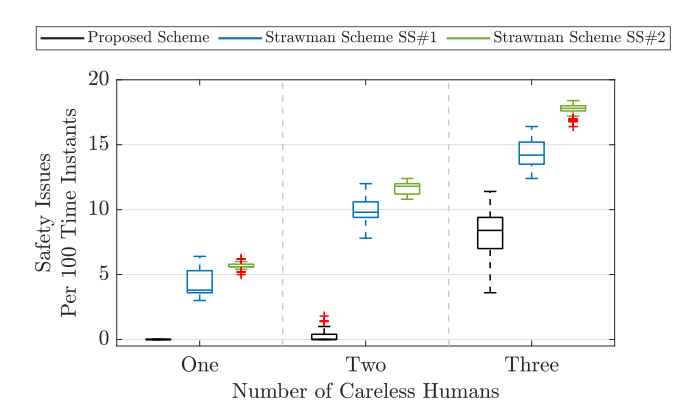


Fig. 7. Packaging line—comparing safety for the proposed scheme, the strawman scheme SS#1, and the strawman scheme SS#2.

Fig. 7) metrics achieved by the proposed robot action planning scheme increase as well. This is understandable, as the combination of two or more careless humans may lead to a wide-range of consequences on the performance metrics.

C. Sensitivity Analysis—Impact of α

In this section, we conducted a sensitivity analysis of the efficiency and safety metrics with respect to the value of α (i.e., the likelihood that a careless human overlooks safety alarms). To carry out this sensitivity analysis, we assumed that there are two careless humans.

Fig. 8 shows how α impacts the efficiency and safety metrics. This figure reports the normalized mean values of 2000 runs, where the values for $\alpha=1$ are used as the normalizing constants. From Fig. 8, we see that as α increases, the performance of the proposed robot action planning scheme slightly degrades. This is consistent with our expectation; as α increases, the likelihood of overlooking safety alarms by careless humans increases, which leads to deviation from the generated optimal plan, and consequently efficiency and safety degradation.

VIII. SIMULATION STUDY—COLLABORATIVE ASSEMBLY

In this section, we investigated the effectiveness of the planning scheme given in Algorithm 1 by simulating and

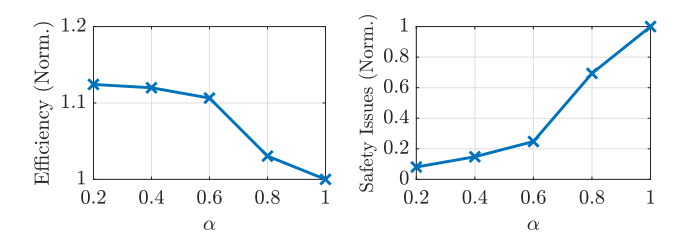
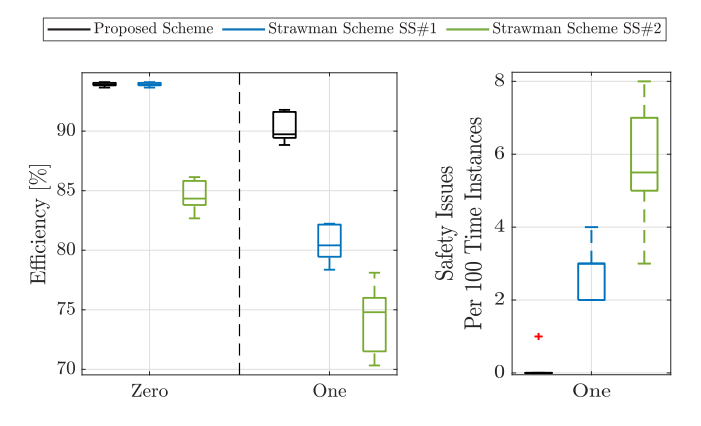


Fig. 8. Packaging line—the impact of α on the obtained mean efficiency and safety metrics.



Number of Careless Humans

Fig. 9. Collaborative assembly—comparing efficiency and safety for the proposed scheme, and for the strawman schemes SS#1 and SS#2.

testing it on a collaborative assembly line with two humans, which is discussed in Section III-B. In the simulated scenario, the robot should provide three pieces for each human, i.e., $\eta = 3$.

System parameters were $\mu_1^1 = \mu_1^3 = \mu_2^3 = 5$, $\mu_1^2 = 4$, $\mu_2^1 = 6$, $\mu_2^2 = 7$, $\sigma_1^1 = \sigma_1^2 = 1$, $\sigma_1^3 = \sigma_2^1 = \sigma_2^2 = 1.5$, $\sigma_2^3 = 2$, $\underline{\lambda}_1^1 = \underline{\lambda}_1^2 = \underline{\lambda}_1^3 = \underline{\lambda}_2^3 = 3$, $\underline{\lambda}_2^1 = \underline{\lambda}_2^2 = \overline{\lambda}_1^2 = 5$, $\overline{\lambda}_1^1 = \overline{\lambda}_1^3 = \overline{\lambda}_2^1 = \overline{\lambda}_2^3 = 7$, $\overline{\lambda}_2^2 = 9$, G = 3, K = 30, and $\ell_i^j = 2 \ \forall i, j$. We assumed that objective function $f_1(\cdot)$ is more important than objective function $f_2(\cdot)$; hence, we set $\theta_1 = 1$ and $\theta_2 = 0.5$. Also, we assumed that the probability that a careless human overlooks safety alarms is 50%, i.e., $\alpha_1 = \alpha_2 = 0.5$.

Fig. 9 presents the achieved efficiency (left figure) as defined in (17) and the number of safety issues per 100 time instances (right figure) for strawman schemes (i.e., SS#1 [23] and SS#2 [79]) and for the proposed robot action planning scheme. Note that we used 2000 experiments to plot this figure, where the careless human in each experiment has been selected randomly at the beginning of the experiment. Also, the initial state of the human h_i is selected uniformly from the set $\{s_i^1, s_i^{1'}, \dots, s_i^6, s_i^{6'}\}$.

As seen in Fig. 9-left, across all cases, the proposed robot action planning scheme has 6.14% mean (up to 17.12%) gain over SS#1, and 16.45% mean (up to 30.51%) gain over SS#2 with respect to efficiency. Also, from Fig. 9-right, across all cases, the proposed robot action planning scheme has 96.67% mean (up to 100%) gain over SS#1, and 98.19% mean (up to 100%) gain over SS#2 with respect to safety.

IX. CONCLUSION

This article proposed a robot action planning scheme to improve safety and efficiency when a robot is collaborating with N humans. The proposed scheme contributes to the stateof-the-art by taking into account the carelessness of humans in determination of the robot's actions. The core idea is make the planner less sensitive to the behavior of careless humans. The robot updates its belief about the carelessness of humans by observing their behavior, and exploits this belief in scheduling its future actions so as to reduce the opportunities given to the careless humans to put themselves in danger and degrade the efficiency of the generated plan. Our numerical experiments on a packaging line with four humans and on a collaborative assembly line with two humans confirmed the effectiveness of the proposed robot action planning scheme in improving efficiency and safety. Our results revealed that the proposed scheme has the capability of improving efficiency and safety.

Future research will consider how to update the probability density function (3) to capture changes in humans' behavior as a result of tiredness and/or boredom, and modify the developed scheme to leverage those updates. It will also consider how to extend the presented idea to account for a wide range of careless actions (e.g., dropping the box in a packaging line). We are planning to investigate cases where human's carelessness levels (and possibly the number of careless humans) change during the collaboration. Future work will also discuss how to obtain/identify the actual carelessness level of humans.

ACKNOWLEDGMENT

The authors would like to thank Prof. Jeffrey M. Zacks from the Department of Psychological and Brain Sciences, and Dr. Vladimir P. Kurenok from the Department of Electrical and Systems Engineering, both at the *Washington University in St. Louis*, for their help in conducting the psychological investigations and formulating the problem.

REFERENCES

- A. Isma and B. Brahim, "Time-dependant trajectory generation for teleoperated mobile manipulator," in *Proc. 3rd Int. Conf. Control, Eng. Inf. Technol.*, Tlemcen, Algeria, 2015, pp. 1–5.
- [2] A. Mortl, M. Lawitzky, A. Kucukyilmaz, M. Sezgin, C. Basdogan, and S. Hirche, "The role of roles: Physical cooperation between humans and robots," *Int. J. Robot. Res.*, vol. 31, no. 13, pp. 1656–1674, Aug. 2012.
- [3] J. A. Marvel, J. Falco, and I. Marstio, "Characterizing task-based human-robot collaboration safety in manufacturing," *IEEE Trans. Syst.*, *Man, Cybern.*, *Syst.*, vol. 45, no. 2, pp. 260–275, Feb. 2015.
- [4] K. Baraka, S. Rosenthal, and M. Veloso, "Enhancing human understanding of a mobile robot's state and actions using expressive lights," in *Proc. 25th IEEE Int. Symp. Robot Hum. Interact. Commun.*, 2016, pp. 652–657.
- [5] M. S. Wogalter, "Communication-human information processing (C-HIP) model in forensic warning analysis," in *Proc. 20th Congr. Int. Ergon. Assoc.*, 2018, pp. 761–769.
- [6] X. Broquere, D. Sidobre, and I. Herrera-Aguilar, "Soft motion trajectory planner for service manipulator robot," in *Proc. IEEE/RSJ Int. Conf. Intell. Robot. Syst.*, Nice, France, 2008, pp. 2808–2813.
- [7] A. M. Zanchettin, N. M. Ceriani, P. Rocco, H. Ding, and B. Matthias, "Safety in human-robot collaborative manufacturing environments: Metrics and control," *IEEE Trans. Autom. Sci. Eng.*, vol. 13, no. 2, pp. 882–893, Apr. 2016.

- [8] A. D. Luca and F. Flacco, "Integrated control for pHRI: Collision avoidance, detection, reaction and collaboration," in *Proc. 4th IEEE RAS* & EMBS Int. Conf. Biomed. Robot. Biomechatron., Rome, Italy, 2012, pp. 288–295.
- [9] G. B. Avanzini, N. M. Ceriani, A. M. Zanchettin, P. Rocco, and L. Bascetta, "Safety control of industrial robots based on a distributed distance sensor," *IEEE Trans. Control Syst. Technol.*, vol. 22, no. 6, pp. 2127–2140, Nov. 2014.
- [10] M. Makarov, A. Caldas, M. Grossard, P. Rodríguez-Ayerbe, and D. Dumur, "Adaptive filtering for robust proprioceptive robot impact detection under model uncertainties," *IEEE/ASME Trans. Mechatron.*, vol. 19, no. 6, pp. 1917–1928, Dec. 2014.
- [11] S. Lu, J. H. Chung, and S. A. Velinsky, "Human-robot collision detection and identification based on wrist and base force/torque sensors," in *Proc. IEEE Int. Conf. Robot. Autom.*, Barcelona, Spain, 2005, pp. 3796–3801.
- [12] B. Schmidt and L. Wang, "Depth camera based collision avoidance via active robot control," *J. Manuf. Syst.*, vol. 33, no. 4, pp. 711–718, Oct. 2014.
- [13] G. Soter, A. Conn, H. Hauser, and J. Rossiter, "Bodily aware soft robots: Integration of proprioceptive and exteroceptive sensors," in *Proc. IEEE Int. Conf. Robot. Autom.*, Brisbane, QLD, Australia, 2018, pp. 2448–2453.
- [14] S. Haddadin, A. Albu-Schaffer, A. D. Luca, and G. Hirzinger, "Collision detection and reaction: A contribution to safe physical human-robot interaction," in *Proc. IEEE/RSJ Int. Conf. Intell. Robot. Syst.*, Nice, France, 2008, pp. 3356–3363.
- [15] S. Parusel, S. Haddadin, and A. Albu-Schaffer, "Modular state-based behavior control for safe human-robot interaction: A lightweight control architecture for a lightweight robot," in *Proc. IEEE Int. Conf. Robot. Autom.*, Shanghai, China, 2011, pp. 4298–4305.
- [16] Y. Shi, Y. Huang, D. Minnen, A. Bobick, and I. Essa, "Propagation networks for recognition of partially ordered sequential action," in *Proc. IEEE Comput. Soc. Conf. Comput. Vis. Pattern Recognit.*, 2004, pp. 862–869.
- [17] M. Albanese, R. Chellappa, V. Moscato, A. Picariello, V. S. Subrahmanian, and P. Turaga, "A constrained probabilistic Petri Net framework for human activity detection in video," *IEEE Trans. Multimedia*, vol. 10, no. 6, pp. 982–996, Oct. 2008.
- [18] J. Kinugawa, A. Kanazawa, S. Arai, and K. Kosuge, "Adaptive task scheduling for an assembly task coworker robot based on incremental learning of human's motion patterns," *IEEE Robot. Autom. Lett.*, vol. 2, no. 2, pp. 856–863, Apr. 2017.
- [19] D. Vasquez, T. Fraichard, and C. Laugier, "Incremental learning of statistical motion patterns with growing hidden Markov models," *IEEE Trans. Intell. Transp. Syst.*, vol. 10, no. 3, pp. 403–416, Sep. 2009.
- [20] B. T. Morris and M. M. Trivedi, "Trajectory learning for activity understanding: Unsupervised, multilevel, and long-term adaptive approach," *IEEE Trans. Pattern Anal. Mach. Intell.*, vol. 33, no. 11, pp. 2287–2301, Nov. 2011.
- [21] K. Li, J. Hu, and Y. Fu, "Modeling complex temporal composition of actionlets for activity prediction," in *Proc. 12th Eur. Conf. Comput. Vis.*, Florence, Italy, 2012, pp. 286–299.
- [22] H. Ding, M. Schipper, and B. Matthias, "Optimized task distribution for industrial assembly in mixed human-robot environments—Case study on IO module assembly," in *Proc. IEEE Int. Conf. Autom. Sci. Eng.*, Taipei, Taiwan, 2014, pp. 19–24.
- [23] K. P. Hawkins, N. Vo, S. Bansal, and A. F. Bobick, "Probabilistic human action prediction and wait-sensitive planning for responsive humanrobot collaboration," in *Proc. 13th IEEE-RAS Int. Conf. Human. Robot.*, Atlanta, GA, USA, 2013, pp. 499–506.
- [24] K. P. Hawkins, S. Bansal, N. N. Vo, and A. F. Bobick, "Anticipating human actions for collaboration in the presence of task and sensor uncertainty," in *Proc. IEEE Int. Conf. Robot. Autom.*, Hong Kong, China, 2014, pp. 2215–2222.
- [25] Y. Tanaka, J. Kinugawa, and K. Kosuge, "Motion planning with worker's trajectory prediction for assembly task partner robot," in *Proc. IEEE/RSJ Int. Conf. Intell. Robot. Syst.*, Vilamoura, Portugal, 2012, pp. 1525–1532.
- [26] A. Kanazawa, J. Kinugawa, and K. Kosuge, "Adaptive motion planning for a collaborative robot based on prediction uncertainty to enhance human safety and work efficiency," *IEEE Trans. Robot.*, vol. 35, no. 4, pp. 817–832, Aug. 2019.
- [27] K. Baizid, A. Yousnadj, A. Meddahi, R. Chellali, and J. Iqbal, "Time scheduling and optimization of industrial robotized tasks based on genetic algorithms," *Robot. Comput.-Integr. Manuf.*, vol. 34, pp. 140–150, Aug. 2015.

- [28] M. Vasic and A. Billard, "Safety issues in human-robot interactions," in *Proc. IEEE Int. Conf. Robot. Autom.*, Karlsruhe, Germany, 2013, pp. 197–204.
- [29] B. S. Dhillon, Robot System Reliability and Safety: A Modern Approach. Boca Raton, FL, USA: CRC Press, 2015.
- [30] I. Cabanes, A. Zubizarreta, C. Pinto, F. Artaza, M. Marcos, and O. Altuzarra, "Multidisciplinary project-based learning of robotics," in Service Robots and Robotics: Design and Application, M. Ceccarelli, Ed. Pennsylvania, PA, USA: IGI Global, 2012, ch. 6, pp. 92–104.
- [31] M. Botvinick and D. C. Plaut, "Doing without schema hierarchies: A recurrent connectionist approach to normal and impaired routine sequential action," *Psychol. Rev.*, vol. 111, no. 2, pp. 395–429, Apr. 2004.
- [32] M. M. Botvinick and L. M. Bylsma, "Distraction and action slips in an everyday task: Evidence for a dynamic representation of task context," *Psychon. Bull. Rev.*, vol. 12, no. 6, pp. 1011–1017, Dec. 2005.
- [33] J. Carlson and R. R. Murphy, "How UGVs physically fail in the field," IEEE Trans. Robot., vol. 21, no. 3, pp. 423–437, Jun. 2005.
- [34] E. I. Barakova, P. Bajracharya, M. Willemsen, T. Lourens, and B. Huskens, "Long-term LEGO therapy with humanoid robot for children with ASD," Expert Syst., vol. 32, no. 6, pp. 698–709, Dec. 2015.
- [35] S. Ehret, S. Roth, S. U. Zimmermann, A. Selter, and R. Thomaschke, "Feeling time in nature: The influence of directed and undirected attention on time awareness," *Appl. Cogn. Psychol.*, vol. 34, no. 3, pp. 737–746, May/Jun. 2020.
- [36] L. Itti, G. Rees, and J. K. Tsotsos, Neurobiology of Attention. Cambridge, MA, USA: Academic, 2005.
- [37] R. M. Enoka and J. Duchateau, "Muscle fatigue: what, why and how it influences muscle function," *J. Physiol.*, vol. 586, no. 1, pp. 11–23, Jan. 2008.
- [38] L. Peternel, N. Tsagarakis, D. Caldwell, and A. Ajoudani, "Robot adaptation to human physical fatigue in human-robotco-manipulation," *Auton. Robot.*, vol. 42, no. 5, pp. 1011–1021, Nov. 2017.
- [39] R. M. Klein, "Inhibition of return," Trends Cogn. Sci., vol. 4, no. 4, pp. 138–147, Apr. 2000.
- [40] M. Huber, A. Knoll, T. Brandt, and S. Glasauer, "When to assist?— Modelling human behaviour for hybrid assembly systems," in *Proc. 41st Int. Symp. Robot. 6th German Conf. Robot.*, Munich, Germany, 2010, pp. 1–6.
- [41] H. Ding, G. Reibig, K. Wijaya, D. Bortot, K. Bengler, and O. Stursberg, "Human arm motion modeling and long-term prediction for safe and efficient human-robot-interaction," in *Proc. IEEE Int. Conf. Robot. Autom.*, Shanghai, China, 2011, pp. 5875–5880.
- [42] H. B. Amor, G. Neumann, S. Kamthea, O. Kroemer, and J. Peters, "Interaction primitives for human-robot cooperation tasks," in *Proc. IEEE Int. Conf. Robot. Autom.*, Hong Kong, China, 2014, pp. 2831–2837.
- [43] H. S. Koppula and A. Saxena, "Anticipating human activities for reactive robotic response," in *Proc. IEEE/RSJ Int. Conf. Intell. Robot. Syst.*, Tokyo, Japan, 2013, p. 2071.
- [44] J. F. Fisac et al., "Probabilistically safe robot planning with confidence-based human predictions," in *Proc. Robot., Sci. Syst.*, Pittsburgh, PA, USA, 2018, pp. 1–9.
- [45] A. Bajcsy et al., "A scalable framework for real-time multi-robot, multihuman collision avoidance," in *Proc. Int. Conf. Robot. Autom.*, Montreal, QC, Canada, 2019, pp. 936–943.
- [46] K. P. Hawkins and P. Tsiotras, "Anticipating human collision avoidance behavior for safe robot reaction," in *Proc. IEEE Conf. Decis. Control*, Miami Beach, FL, USA, 2018, pp. 6301–6306.
- [47] X. Yu, W. He, Y. Li, C. Xue, J. Li, J. Zou, and C. Yang, "Bayesian estimation of human impedance and motion intention for human-robot collaboration," *IEEE Trans. Control Syst. Technol.*, vol. 51, no. 4, pp. 1822–1834, Apr. 2021.
- [48] Z. Jin and P. R. Pagilla, "Shared control with efficient subgoal identification and adjustment for human–robot collaborative tasks," *IEEE Trans. Control Syst. Technol.*, vol. 30, no. 1, pp. 326–335, Jan. 2022.
- [49] L. Chen, M. Wu, M. Zhou, Z. Liu, J. She, and K. Hirota, "Dynamic emotion understanding in human–robot interaction based on two-layer fuzzy SVR-TS model," *IEEE Trans. Syst., Man, Cybern., Syst.*, vol. 50, no. 2, pp. 490–501, Feb. 2020.
- [50] Z. Jin, P. R. Pagilla, H. Maske, and G. Chowdhary, "Task learning, intent prediction, and adaptive blended shared control with application to excavators," *IEEE Trans. Control Syst. Technol.*, vol. 29, no. 1, pp. 18–28, Jan. 2021.
- [51] S. Pellegrinelli, H. Admoni, S. Javdani, and S. Srinivasa, "Human-robot shared workspace collaboration via hindsight optimization," in *Proc. IEEE/RSJ Int. Conf. Intell. Robot. Syst.*, Daejeon, South Korea, 2016, pp. 831–838.

- [52] S. Javdani, H. Admoni, S. Pellegrinelli, S. Srinivasa, and J. A. Bagnell, "Shared autonomy via hindsightoptimization for teleoperation and teaming," *Int. J. Robot. Res.*, vol. 37, no. 7, pp. 717–742, Jun. 2018.
- [53] V. V. Unhelkar, S. Li, and J. A. Shah, "Semi-supervised learning of decision-making models for human-robot collaboration," in *Proc. Conf. Robot Learn.*, 2020, pp. 192–203.
- [54] Y. Cheng, L. Sun, C. Liu, and M. Tomizuka, "Towards efficient human-robot collaboration with robust plan recognition and trajectory prediction," *IEEE Robot. Autom. Lett.*, vol. 5, no. 2, pp. 2602–2609, Apr. 2020.
- [55] S. Nikolaidis, R. Ramakrishnan, K. Gu, and J. Shah, "Efficient model learning from joint-action demonstrations for human-robot collaborative tasks," in *Proc. 10th Annu. ACM/IEEE Int. Conf. Hum. Robot Interact.*, Portland, OR, USA, 2015, pp. 189–196.
- [56] M. Chen, S. Nikolaidis, H. Soh, D. Hsu, and S. Srinivasa, "Trust-aware decision making for human-robot collaboration: Model learning and planning," ACM Trans. Hum. Robot Interact., vol. 9, no. 2, pp. 1–23, Feb. 2020.
- [57] M.-L. Lee, W. Liu, S. Behdad, X. Liang, and M. Zheng, "Robot-assisted disassembly sequence planning with real-time human motion prediction," *IEEE Trans. Syst., Man, Cybern., Syst.*, vol. 53, no. 1, pp. 438–450, Jan. 2023.
- [58] J. Hwang, J. Kim, A. Ahmadi, M. Choi, and J. Tani, "Dealing with large-scale spatio-temporal patterns in imitative interaction between a robot and a human by using the predictive coding framework," *IEEE Trans. Syst., Man, Cybern., Syst.*, vol. 50, no. 5, pp. 1918–1931, May 2020.
- [59] R. Wilcox, S. Nikolaidis, and J. Shah, "Optimization of temporal dynamics for adaptive human-robot interaction in assembly manufacturing," in *Proc. Robot., Sci. Syst.*, Sydney, NSW, Australia, 2012, pp. 441–448.
- [60] X. Xing, J. Xia, D. Huang, and Y. Li, "Path learning in human-robot collaboration tasks using iterative learning methods," *IEEE Trans. Control Syst. Technol.*, vol. 30, no. 5, pp. 1946–1959, Sep. 2022.
- [61] S. Lyu and C. C. Cheah, "Human-robot interaction control based on a general energy shaping method," *IEEE Trans. Control Syst. Technol.*, vol. 28, no. 6, pp. 2445–2460, Nov. 2020.
- [62] F. Belkhouche, "Reactive path planning in a dynamic environment," IEEE Trans. Robot., vol. 25, no. 4, pp. 902–911, Aug. 2009.
- [63] G. S. Aoude, B. D. Luders, J. M. Joseph, N. Roy, and J. P. How, "Probabilistically safe motion planning to avoid dynamic obstacles with uncertain motion patterns," *Auton. Robot.*, vol. 35, pp. 51–76, May 2013.
- [64] I. Ranatunga, F. L. Lewis, D. O. Popa, and S. M. Tousif, "Adaptive admittance control for human-robot interaction using model reference design and adaptive inverse filtering," *IEEE Trans. Control Syst. Technol.*, vol. 25, no. 1, pp. 278–285, Jan. 2017.
- [65] S.-Y. Jiang, C.-Y. Lin, K.-T. Huang, and K.-T. Song, "Shared control design of a walking-assistant robot," *IEEE Trans. Control Syst. Technol.*, vol. 25, no. 6, pp. 2143–2150, Nov. 2017.
- [66] J. Quintas, G. S. Martins, L. Santos, P. Menezes, and J. Dias, "Toward a context-aware human–robot interaction framework based on cognitive development," *IEEE Trans. Syst., Man, Cybern., Syst.*, vol. 49, no. 1, pp. 227–237, Jan. 2019.
- [67] M. Lippi and A. Marino, "Human multi-robot safe interaction: A trajectory scaling approach based on safety assessment," *IEEE Trans. Control Syst. Technol.*, vol. 29, no. 4, pp. 1565–1580, Jul. 2021.
- [68] Y. Huo, X. Li, X. Zhang, X. Li, and D. Sun, "Adaptive intention-driven variable impedance control for wearable robots with compliant actuators," *IEEE Trans. Control Syst. Technol.*, vol. 31, no. 3, pp. 1308–1323, May 2023.
- [69] A. W. Kemp, "Characterizations of a discrete normal distribution," J. Stat. Plan. Inference, vol. 63, no. 2, pp. 223–229, Oct. 1997.
- [70] J. Mattingley, Y. Wang, and S. Boyd, "Receding horizon control," *IEEE Contr. Syst. Mag.*, vol. 31, no. 3, pp. 52–65, Jun. 2011.
- [71] J. Mattingley, Y. Wang, and S. Boyd, "Code generation for receding horizon control," in *Proc. IEEE Int. Symp. Comput.-Aided Control Syst. Des.*, Yokohama, Japan, 2010, pp. 985–992.
- [72] M. P. Chapman et al., "A risk-sensitive finite-time reachability approach for safety of stochastic dynamic systems," in *Proc. Am. Control Conf.*, Philadelphia, PA, USA, 2019, pp. 2958–2963.
- [73] D. Fridovich-Keil et al., "Confidence-aware motion prediction for real-time collision avoidance," *The Int. J. Robot. Res.*, vol. 39, nos. 2–3, pp. 250–265, Mar. 2020.
- [74] J. Xu, J. Wang, and W. Chen, "An efficient recharging task planning method for multi-robot autonomous recharging problem," in *Proc. IEEE Int. Conf. Robot. Biomimet.*, Dali, China, 2019, pp. 1839–1844.
- [75] S. P. Boyd and L. Vandenberghe, Convex Optimization. Cambridge, MA, USA: Cambridge Univ. Press, 2004.

- [76] X. Yang, Nature-Inspired Optimization Algorithms. Cambridge, MA, USA: Academic, 2014.
- [77] M. A. Gennert and A. L. Yuille, "Determining the optimal weights in multiple objective function optimization," in *Proc. 2nd Int. Conf. Comput. Vis.*, Tampa, FL, USA, 1988, pp. 87–89.
- [78] M. Schlueter, J. Egea, and J. Banga, "Extended ant colony optimization for non-convex mixed integer nonlinear programming," *Comput. Oper. Res.*, vol. 36, no. 7, pp. 2217–2229, 2009.
- 79] M. Ryan, "Constraint-based multi-robot path planning," in *Proc. IEEE Int. Conf. Robot. Autom.*, 2010, pp. 922–928.



Mehdi Hosseinzadeh (Senior Member, IEEE) received the Ph.D. degree in electrical engineering from the University of Tehran, Tehran, Iran, in 2016.

From 2017 to 2019, he was a Postdoctoral Researcher with the Université Libre de Bruxelles, Brussels, Belgium. From October 2018 to December 2018, he was a Visiting Researcher with the University of British Columbia, Vancouver, BC, Canada. From 2019 to 2022, he was a Postdoctoral Research Associate with Washington University in St. Louis, St. Louis, MO, USA. He is currently an

Assistant Professor with the School of Mechanical and Materials Engineering, Washington State University, Pullman, WA, USA. His research focuses on safety, resilience, and long-term autonomy of autonomous systems, with applications to autonomous robots, human–robot interaction, energy systems, video streaming, and drug delivery systems.



Bruno Sinopoli (Fellow, IEEE) received the Ph.D. degree in electrical engineering from the University of California at Berkeley, Berkeley, CA, USA, in

After a postdoctoral position with Stanford University, Stanford, CA, USA, he was the Faculty with Carnegie Mellon University, Pittsburgh, PA, USA, from 2007 to 2019, where he was a Full Professor with the Department of Electrical and Computer Engineering, courtesy appointments of Mechanical Engineering, and with the Robotics

Institute, Carnegie Mellon University and the Co-Director of the Smart Infrastructure Institute, Carnegie Mellon University. In 2019, he was with Washington University in St. Louis, St. Louis, MO, USA, where he is the Chair of the Electrical and Systems Engineering Department. His research interests include the modeling, analysis and design cyber–physical systems with applications to energy systems, interdependent infrastructures, and Internet of Things.



Aaron F. Bobick (Fellow, IEEE) received the B.S. degree in mathematics and computer science from Massachusetts Institute of Technology (MIT), Cambridge, MA, USA, in 1981, and the Ph.D. degree in cognitive science from MIT in 1987.

In 1987, he was with the Perception Group, Artificial Intelligence Laboratory, SRI International, Menlo Park, CA, USA, and soon after was jointly named a Visiting Scholar with Stanford University, Stanford, CA, USA. From 1992 to July 1999, he served as an Assistant and then an Associate

Professor with the Vision and Modeling Group, Media Laboratory, MIT. From 1999 to 2015, he was with the College of Computing, Georgia Institute of Technology, Atlanta, GA, USA. In 2015, he was a Dean of the School of Engineering and Applied Science, Washington University in St. Louis, St. Louis, MO, USA, and the James M. McKelvey Professor. His research primarily focuses on action recognition by computer vision—a field in which he is a pioneer—and robot perception for human–robot collaboration.